Catalysis Today 245 (2015) 46–53

Contents lists available at ScienceDirect

Catalysis Today

journal homepage: www.elsevier.com/locate/cattod

Photocatalytic and photoelectrocatalytic degradation and mineralization of small biological compounds amino acids at TiO_2 photoanodes

Guiying Li[a,b], Xiaolu Liu[a,b], Jibin An[a,d], Hai Yang[a], Shanqing Zhang[b], Po-Keung Wong[c], Taicheng An[a,*], Huijun Zhao[b,**]

[a] State Key Laboratory of Organic Geochemistry, Guangzhou Institute of Geochemistry, Chinese Academy of Sciences, Guangzhou 510640, China
[b] Centre for Clean Environment and Energy, Gold Coast Campus, Griffith University, Queensland 4222, Australia
[c] School of Life Sciences, The Chinese University of Hong Kong, Shatin, N.T., Hong Kong SAR, China
[d] University of Chinese Academy of Sciences, Beijing 100049, China

ARTICLE INFO

Article history:
Received 18 November 2013
Received in revised form 23 May 2014
Accepted 29 May 2014
Available online 20 July 2014

Keywords:
Photocatalysis
Photoelectrocatalysis
Amino acids
Biological compounds
Mineralization

ABSTRACT

Quantitative evaluation of photocatalytic (PC) and photoelectrocatalytic (PEC) degradation of small biological compounds like amino acids (AAs) were systematically investigated at illuminated nanoparticulate TiO_2 photoanode using a thin-layer photoelectrochemical cell. Three model AAs like phenylalanine (Phe), tyrosine (Tyr) and tryptophan (Trp), were found to be photocatalytically and photoelectrocatalytically degradable. PEC degradation efficiency was much higher than that of PC method for all compounds investigated, and the superiority becomes more obvious at higher concentrations. Organic nitrogen atoms in AAs can be oxidized to either NH_3/NH_4^+ or NO_3^-, or both, depending the chemical structures of AAs and degradation methods used. HPLC analysis found that, for a given AA except Phe, the hydrophilicity characteristics of intermediates are differed slightly between PC and PEC process. For a given method, similar hydrophilicity characteristics were obtained from all AAs investigated except Phe. Theoretically calculated results showed that initial reaction sites for all single-ringed AAs are likely to occur on the atoms within 6-membered ring structure, while for double-ringed AA, the initial reaction sites are likely to occur at 6-membered ring structure (PC) or at 5-membered ring structure (PEC). Both experimental and theoretical results demonstrated PEC reaction mechanisms differed remarkably from that of PC process.

1. Introduction

Over the recent decades, a noticeable increase interest in more effective treatments of wastewater having high loads of nitrogen-containing organic compounds due to the increased pollution to surface water and groundwater [1–9]. There are large numbers of nitrogen-containing compounds exist in the nature. Amino acids (AAs) are a particularly important category of nitrogen-containing compounds, and are also the building block of proteins, with combining the acidic (–COOH) and the basic ($–NH_2$) functional groups together. This category of nitrogen-containing compounds can cause severe water quality problems such as eutrophication, which could lead to the rapid growth of the algae and bacteria in the water and wastewater [10–12]. In addition, AAs can rapidly react with chlorine, chloramines or ozone producing toxic nitrogenous disinfection byproducts (N-DBPs) during water disinfection processes [4,13–17]. Thus, to develop advanced water and wastewater treatment technologies are therefore highly desirable [18–20].

A number of previous studies have suggested that the photocatalytic (PC) oxidation of adsorbed organics at the irradiated semiconductor surface is a primary step. By measuring the zeta potential and ^1H NMR spectroscopy of TiO_2 aqueous suspension systems of seven different AAs, Tran et al. [21] observed that the acidity of TiO_2 surface changed due to the adsorption of AAs on TiO_2 surface. Phenylalanine (Phe) is adsorbed by the amino group, leading to the low photodecomposition rate, while AAs containing –OH (serine), –NH (tryptophan, histidine), or $–NH_2$ (asparagine) appeared to be adsorbed more easily by these side chains, and therefore to be more vulnerable to PC oxidation. However, other researchers [22] proposed that the organics chemisorbed to the catalyst surface is predominantly through the carboxylate oxygen

* Corresponding author. Tel.: +86 20 85291501; fax: +86 20 85290706.
** Corresponding author. Tel.: +61 7 555 2 8261; fax: +61 7 5552 8067.
E-mail addresses: antc99@gig.ac.cn (T. An), h.zhao@griffith.edu.au (H. Zhao).

http://dx.doi.org/10.1016/j.cattod.2014.05.040
0920-5861/

Table 1
Amino acids examined in the present study.

Name	Abbr	Chemical formula	Molecular weight	Abs. λ_{max} (nm)	n_{NH_3}	$n_{NO_3^-}$	$n_{NH_3/HN_4^+}/n_{NO_3^-}$
Phenylalanine	Phe	$C_9H_{11}NO_2$	165.19	257;206;188	40	48	0.833
Tryptophan	Trp	$C_{11}H_{12}N_2O_2$	204.23	280;219	46	62	0.742
Tyrosine	Tyr	$C_9H_{11}NO_3$	181.19	274;222;193	38	46	0.826

* Abbr: abbreviation. Abs.: absorbance. n_{NH_3/HN_4^+} and $n_{NO_3^-}$ are the required number of electron transfer for converting N to NH_3/NH_4^+ and NO_3^-, respectively.

atoms. Recently, by calculating the point charges of all individual atoms in the AAs, Horikoshi et al. [23] confirmed that the point of chemisorption of AAs is mainly through the carboxylate oxygen though there may be a remote possibility of contribution by alcoholic oxygen or other function groups.

For photo-assisted mineralization of organic molecules containing heteroatoms such as nitrogen, N could be converted to NO_3^-, NO_2^- and/or NH_4^+ ions [24]. However, when a N–N bond is present in the original substrate, the production of N_2 gas can be observed as one of the mineralization by-products [25]. The photocatalytic mineralization of AAs normally yields NH_4^+ and NO_3^- ions, depending on the structural fragment bonded to the α-carboxylic acid functional group [23]. The nitrogen in the AAs is typically converted into NH_4^+ ions, and to a lesser extent to NO_3^-, while carbon atoms are converted into CO_2, as demonstrated by Hidaka and co-workers' work. They [26] investigated the PC mineralization of a series of AAs at TiO_2 photocatalysis surface illuminated with UVA and UVB by measuring the CO_2 evolution and the conversion of the amine group to NH_4^+ and NO_3^- ions. PC degradation mechanisms of a number of AAs have been proposed. TiO_2 surface electrons and surface •OH radicals can react with AAs and lead to deamination to give NH_3. While the reaction with •OH, HO_2• lead to formation of CO_2 in various pathways. The same research group [23] carried out a more detailed research on PC degradation pathway of three AAs L-serine, L-phenylalanine and L-alanine based on the experiment and molecular orbital calculations. They found that the rates of the amine loss, of the evolution of CO_2, and of the formation of NH_4^+ and NO_3^- were different widely because of their various side chains on the α-carbon. Fox et al.'s [27] research found that the •OH generated on the TiO_2 surface can competitively attack terminal –COOH and $–NH_2$ groups. Accordingly, they proposed that the α-carbon adjacent to the primary amine is initially oxidized to promote scission of N–C bond, whereas N–C bond in the amide moiety is easily and readily cleaved. Subsequent to cleavage of N–C bond in primary amine homologs, formation of NH_4^+ is fairly rapid and reflects the variation in the number of the methylene groups or chain length. While Monig et al. [28] suggested that the positive charge of $[NH_3]^+$– mediates the attacking electrophilic •OH radical to C–H bonds located further away from the α-carbon. To date, all reports on PC degradation of AAs were conducted in TiO_2 particle suspension systems. No published work on the photoelectrocatalytic (PEC) degradation of the AAs can be found in the literature.

The main objectives of this work are first to quantitatively compare the efficiencies of PC and PEC degradation of AAs, and second to gain a better understanding on the mechanistic pathways of PC and PEC degradation of AAs and the differences between the two techniques. The former provides information to enable the selection of an effective AAs removal technique (e.g., PC or PEC), and the later provides useful information, facilitating mechanistic understanding of PC and PEC degradation of larger biological molecules such as proteins because AAs are the building block of such larger biological molecules. In order to achieve these objectives, we systematically compared PC and PEC degradation of three representative AAs, phenylalanine (Phe), tyrosine (Tyr) and tryptophan (Trp), at illuminated nanoparticulate TiO_2 photoanode using a specially designed thin-layer photoelectrochemical cell. A HPLC system equipped with a photo-diode-array (PDA) detector was employed to obtain the information of PC and PEC degradation products. The frontier electron densities (FEDs) of all test AAs were calculated to predict the initial reaction site/position on AAs via electron extraction (direct photohole reaction in PEC process) and •OH (or equivalent) attack (PC process) mechanisms.

2. Materials and methods

2.1. Chemicals and materials

Indium tin oxide conducting glass slides (ITO, 8 Ω/square) were purchased from Delta Technologies Ltd. (USA). Titanium butoxide (97%, Aldrich), three AAs examined in this study (Table 1) were supplied by Sigma and used as received. Other chemicals used were of analytical grade and purchased from Aldrich unless otherwise stated. All solutions were prepared using high purity deionized water (Millipore Corp., 18 MΩ cm).

2.2. Procedures

The procedures used for TiO_2 colloids preparation and TiO_2 photoanodes fabrication were the same as described in our previous study [29]. Both PC and PEC degradation experiments were performed under identical UV intensity using the same UV-LED/TiO_2 thin-layer photoelectrochemical cell [30]. For PEC degradation experiments, a 2.0 M $NaNO_3$ solution was used as the supporting electrolyte. For the exhaustive degradation experiment, a sample containing various concentrations of AAs and 2.0 M $NaNO_3$ was injected into the thin-layer cell via a precision pump before the degradation process and then subjected to PC and PEC oxidation. For samples need HPLC analysis after oxidation, a continuous sample injection model via a precision pump during the degradation process was used. Under such conditions, the reaction time of a sample was controlled by adjusting the flow rate. A sufficient volume of the reacted sample was collected for further analyses after the system reaching its steady-state for which the collected sample had been subjected to the same reaction time. A 2.0 M $NaNO_3$ solution was used to clean the cell between the two sample injections. PC degradation experiments were conducted under identical experimental conditions as PEC experiments, except the electrochemical system was disconnected.

For PC and PEC experiments, the extent of the mineralization was determined by measuring the charge originated from the oxidation of AAs using PeCOD^{TM} technique [29,31,32]. Fig. S1 illustrates the quantification method of the net charge (Q_{net}) that is originated from PEC degradation of AAs. Fig. S2 shows the quantification method of the net charge (ΔQ_{net}) that is due to PC degradation of AAs. And the detailed information was described in Supporting Information.

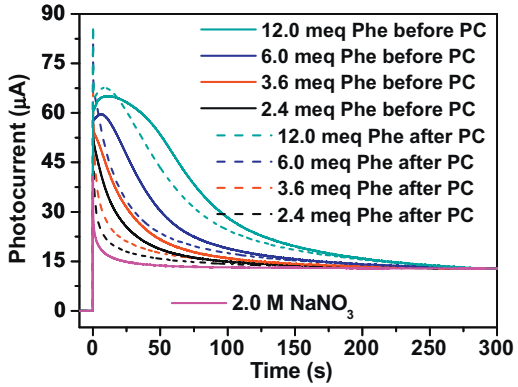

Fig. 1. Typical photocurrent–time profiles of different phenylalanine (Phe) concentrations in the thin-layer photoelectrochemical cell (electrolyte concentration: 2.0 M $NaNO_3$; light intensity: 8.0 mW/cm^2; applied potential bias: +0.30 V (vs. Ag/AgCl)).

2.3. Analysis

Intermediate degradation products were analyzed using a Waters 996 HPLC/MS (Micromass, Manchester, UK) equipped with a photo-diode array detector (PDA) detector and electro-spray ionization (ESI) source. The elution was carried out using a Gemini-NX C18 column (Phenomenex, USA). The separation of AAs and the intermediates was performed with isocratic elution using a 42%:20%:38% by volume of water, methanol and acetonitrile. The eluent flow rate was maintained at 1 ml/min. Nitrogen was used as nebulizer and dry gas. The PDA detection wavelength was set between 191 and 400 nm for acquiring chromatograms and quantitative analysis. The mass spectrum was obtained from 50 to 300 m, and the mass spectrometer was operated in positive ion mode. The cone voltage is 30 V for each of the sample.

2.4. Frontier electron densities calculations

The molecular orbital (MO) calculations were carried out by using Gaussian 03 program (Gaussian, Inc.) at the single determinant (HF/3-21) level with the optimal conformation having minimum energy obtained at the B3LYP/6-31G* level. The FEDs of the highest occupied molecular orbital (HOMO) and the lowest unoccupied molecular orbital (LUMO) were calculated, and the values of $2FED^2_{HOMO}$ and $(FED^2_{HOMO} + FED^2_{LUMO})$ was obtained to predict the reaction sites of electron extraction and radical attack, respectively [33,34].

3. Results and discussion

3.1. Photocatalytic degradation

It is well known that AAs contain organic nitrogen that can be converted to different oxidation states (i.e., HN_3/NH_4^+ and NO_3^-). For this work, the mineralization percentages were calculated by assigning the measured charge transfer to the mineralization products with organic nitrogen being 100% converted to NH_3/NH_4^+ or NO_3^-. Table 1 summaries the number of electron transfer required for mineralizing organic nitrogen of three representative AAs to NH_3/NH_4^+ (n_{NH_3/HN_4^+}) and NO_3^- ($n_{NO_3^-}$). It is obvious that the extent of mineralization could be strongly influenced by the final mineralization products of the organic nitrogen because for a given amino acid, the numbers of electron transfer required to convert the organic nitrogen to NH_3 and NO_3^- are dramatically different.

Fig. 1 shows a set of typical photocurrent–time profiles obtained from Phe solution before and after PC treatment. These

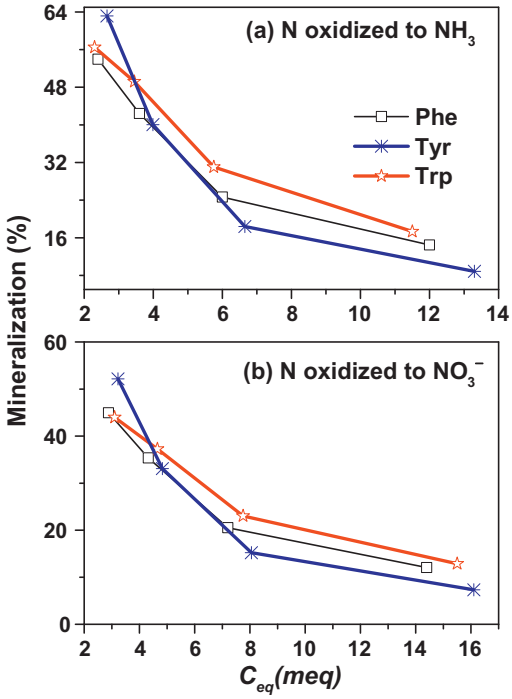

Fig. 2. Photocatalytic degradation of phenylalanine (Phe), tyrosine (Tyr) and tryptophan (Trp): Mineralization percentage against C_{eq} for N oxidized to (a) NH_3 and (b) to NO_3^-.

photocurrent profiles are used to obtain the percentage mineralization of PC treated samples by measuring the amount of electrons lost during PC treatment in accordance with Eqs. (S7)–(S10) in Supporting information. Fig. 2 shows the plots of the mineralization percentage of PC treated samples against the equivalent electron concentration (C_{eq}) for organic nitrogen mineralized to NH_3/NH_4^+ and NO_3^-. All samples were photocatalytically treated for 300 s under 8.0 mW/cm^2 UV light intensity. The equivalent electron concentrations were calculated according to $C_{eq} = n_{NH_3/HN_4^+} \cdot C_M$ for Fig. 2a and $C_{eq} = n_{NO_3^-} \cdot C_M$ for Fig. 2b, respectively, where C_M is the molar concentration of the AAs. The use of C_{eq} allows a more meaningful comparison among different AAs because such a non-characteristic concentration unit represents the electron demands for complete mineralization [30]. More importantly, the electron demand for a given C_{eq} is the same for all AAs, regardless of their chemical structures and electron transfer numbers [30]. For all cases investigated, an increase in the C_{eq} led to a decrease in the mineralization percentage for converting organic nitrogen to both NH_3/NH_4^+ and NO_3^-. However, Tyr exhibited a higher mineralization percentage at lower concentration but lower mineralization percentage at higher concentrations than the other two AAs. The mineralization percentage values and the effect of C_{eq} on these values for Phe and Trp were very similar, except that Trp had higher mineralization percentage values at all tested concentration.

These results are agreed well with other reported results [35]. Table S1 summarized the general susceptibility of an amino acid side chain toward oxidation by •OH. It shows that Trp is to be 1.9-fold more reactive to initial attack. While other researchers found that Trp was the most reactive non-sulfur containing residue and was about 1.6-fold as reactive as Phe in their examination [35]. The reactivity of Trp, Tyr, and Phe, are ca. 17-, 12-, and 11-fold that of Pro [35]. Hidaka et al. found that it would take ca. 5 h of PC reaction for Phe to lose the aromaticity, whereas loss of aromaticity in Trp is almost complete within 2 h irradiation [26].

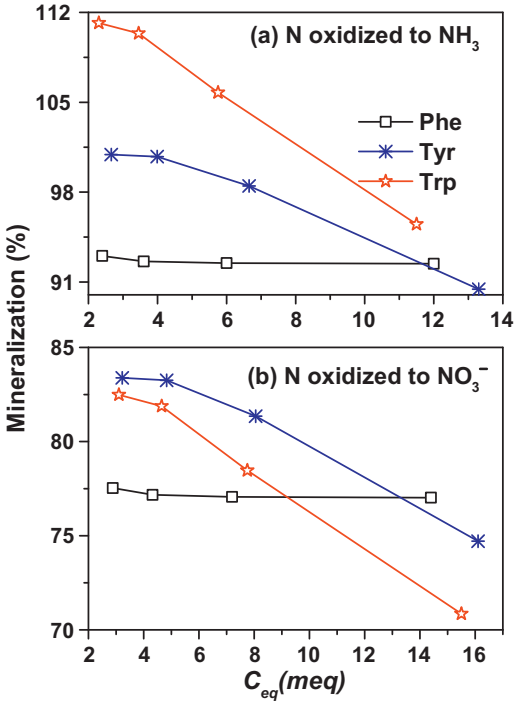

Fig. 3. Photoelectrocatalytic degradation of Phe, Tyr and Trp. (a) Mineralization percentage against C_{eq} for N oxidized to NH_3 and (b) to NO_3^-.

3.2. Photoelectrocatalytic degradation

All samples were photoelectrocatalytically treated under the same conditions as PC except with an applied potential bias of +0.30 V vs. Ag/AgCl. Fig. S3 shows a set of typical photocurrent–time profiles obtained from Trp solution during PEC treatment. These photocurrent profiles are used to obtain the percentage mineralization of PEC treated solution by measuring the amount of electrons lost during PEC treatment in accordance with Eqs. (S1) and (S6) in Supporting information. Fig. 3 shows the plots of the mineralization percentage of PEC treated samples against C_{eq} for organic nitrogen mineralized to NH_3/NH_4^+ and NO_3^-. In general, the mineralization efficiencies of all PEC treated samples converting to both HN_3/NH_4^+ and NO_3^- were found to be much higher than those of PC treated samples under the same experimental conditions, suggesting a superior PEC degradation capability. In strong contrast to PC treated samples, the effect of concentration on Phe mineralization percentage was found to be insignificant, while for Tyr and Trp, the mineralization percentage decreased as the C_{eq} was increased. For Tyr and Trp converting to NH_3/NH_4^+ within lower concentration range (i.e., C_{eq} < 11 meq of electrons), the observed mineralization percentages were higher than that of Phe (Fig. 3a). For Tyr and Trp converting to NH_3/NH_4^+, the mineralization percentages obtained from lower concentration range followed an order of Trp > Tyr > Phe (Fig. 3a). Similarly, for Tyr and Trp converting to NO_3^- within lower concentration range (i.e., C_{eq} < 8 meq of electrons), the observed mineralization percentages were higher than those of Phe (Fig. 3b). However, a completely reversed order of Tyr > Trp within the entire concentration investigated range was observed for converting to NO_3^- (Fig. 3b).

This result can be confirmed by previous reference [36], which is due to the electron-rich nature of indole that can be easily oxidized. The heterocyclic N atom in pyrrole is converted predominantly to NH_4^+ ions. Concomitantly, NO_3^- ions are also gradually produced in smaller quantities [36]. It should be noted that obtained mineralization percentage of Trp within lower concentration range (i.e., <6 meq of electrons) for converting to NH_3/NH_4^+ was greater than

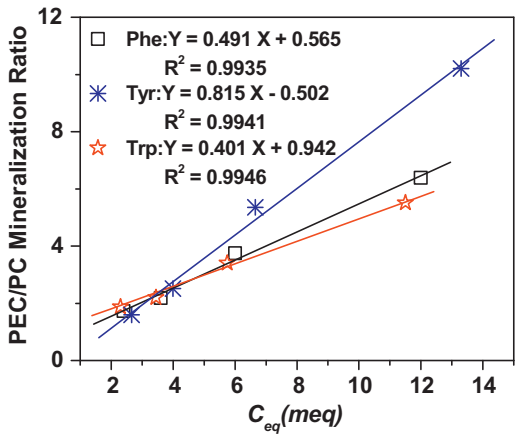

Fig. 4. A plot of PEC to PC mineralization ratio against C_{eq} for Phe, Tyr and Trp.

100%. This suggests that at least some organic nitrogen contents in Trp were converted to NO_3^- during PEC treatment. Theoretically, the electron transfer number ratio ($n_{NH_3/HN_4^+}/n_{NO_3^-}$) follows an order of Phe > Tyr > Trp (Table 1). Such a ratio reflects the carbon to nitrogen ratio and their oxidation states in original AAs, determines the required amount of electron transfer to achieve the same extent of mineralization under PEC conditions. Interestingly, the observed mineralization percentages of this group compound followed the same order of Phe > Tyr > Trp, within low to medium concentration ranges for converting to both NH_3/NH_4^+ and NO_3^-. This suggests that for a given amount of electron transfer, the extent of mineralization is highly dependent on the nitrogen contents and their oxidation states in the original AAs. These observed characteristics are distinctively different from those observed from PC treated samples where no clear pattern or decisive relationship between the $n_{NH_3/HN_4^+}/n_{NO_3^-}$ ratio and the mineralization percentage. This may imply that the organic nitrogen converting to NH_3/NH_4^+ was dominant process.

The differences between PEC and PC in respect to the effect of substrate concentration on the extent of mineralization were quantitatively evaluated by plotting the PEC/PC mineralization ratio against the C_{eq} (Fig. 4). Surprisingly, linear relationships were obtained for all cases investigated. Such liner relationships reveal the superiority (in terms of mineralization efficiency) of PEC over PC method increases as the concentration increases. Furthermore, the slope of the curve quantifies the degree of the superiority of PEC method over PC method in respect to concentration change. The obtained slops were found to follow an order of Tyr (0.815 meq^{-1}) >Phe (0.491 meq^{-1}) > Trp (0.401 meq^{-1}). This again suggests that the carbon to nitrogen ratio and their oxidation states in the original AAs determines the PEC/PC mineralization efficiency. These results also suggest that the characteristics of PEC degradation process differ markedly from PC degradation process. Such differences could be due to the reaction pathway differences between the two processes that deserve a further investigation.

3.3. Frontier electron densities

The PC and PEC degradation results of AAs obtained above have clearly demonstrated different degradation behavior in two processes, which could be due to the mechanistic pathway differences. It is well known that, when TiO_2 nanoparticles were illuminated by UV light with wavelength of less than 400 nm, the photo-induced e^- and h^+ could be created. Moreover, these the h^+ could further react with hydroxyl ions or water to form active oxidative radicals, for example $^{\bullet}OH$ [18]. Therefore, in the PC degradation process, active $^{\bullet}OH$ are mainly involved in indirect addition/substitution reaction

[37], and the direct h^+ attack is likely to occur more possible in PEC process than PC process. This could be one of the most important attributes that deviates the mechanistic pathways of PEC process from PC process.

Theoretically calculated FEDs have been recognized as a useful tool to predict initial reaction step [33,34]. More importantly, the obtained values of $2FED^2_{HOMO}$ and $(FED^2_{HOMO} + FED^2_{LUMO})$ can be used to estimate the initial reaction sites for electron extraction (i.e., direct h^+ attack) and radical attack ($^\bullet OH$), respectively [33,34]. The values of $2FED^2_{HOMO}$ and $(FED^2_{HOMO} + FED^2_{LUMO})$ were therefore calculated and used to evaluate the differences in initial reaction steps of PC and PEC processes. Table 2 summarized FEDs calculation results for three representative AAs. For Phe, higher $2FED^2_{HOMO}$ values were obtained at C^4 (0.349) and C^7 (0.322) indicating the initial h^+ attacks are likely to occur on these two carbon atoms. For $^\bullet OH$ attacks, the same carbon atoms, C^4 (0.476) and C^7 (0.484), are also likely to be the possible initial reaction sites according to $(FED^2_{HOMO} + FED^2_{LUMO})$ values.

Similar results were obtained for Tyr where higher probability for h^+ (C^4, 0.359 and C^7, 0.230) to attack carbon atoms, which are the same carbon atoms as Phe. However, based on the $FED^2_{HOMO} + FED^2_{LUMO}$ values, the higher electron density atom is C^6 (0.422) and C^9 (0.413) should be the first sites of $^\bullet OH$ radicals attacked, which is different from h^+ attacked atoms. The probable reason is that the hydroxy group is considered to be an electron donating group, it increase electron density by releasing electrons into a reaction center. As for Trp, the distinguishing structural characteristic is that it contains an indole functional group which is an aromatic heterocyclic organic compound. Thus, it has a bicyclic structure, consisting of a six-membered benzene ring fused to a five-membered nitrogen-containing pyrrole ring. The participation of the nitrogen lone electron pair in the aromatic ring means indole is not a base, and it does not behave like a simple amine. The most reactive position on indole is electrophilic aromatic substitution of C^5, which is 10^{13} times more reactive than benzene, since the pyrrollic ring is the most reactive portion of indole, thus nucleophilic substitution of the carbocyclic (benzene) ring can take place only after N^7, C^6, and C^5 are substituted (http://en.wikipedia.org/wiki/Indole). However, if this indole functional group is existed in Trp structure, the atom with highest electron densities is different from indole. From the FED calculation results of Trp (Table 2), the largest $2FED^2_{HOMO}$ value were found at C^5 (0.292) and C^6 (0.227) atoms. Consequently, it seems that the C^5 or C^6 atoms should be the possible sites at which the first electron is extracted. While the position of $^\bullet OH$ attack on Trp structure can be inferred from the theoretical calculations results of $FED^2_{HOMO} + FED^2_{LUMO}$, and C^9 (0.350) and C^{12} (0.383) atoms bear the largest electron densities and thus are most prone to be attacked by $^\bullet OH$; and C^6 also has significant electron densities. This calculation result is agreed with other researchers' experimental analysis very well, which suggested that $^\bullet OH$ can interact with the benzene moiety of Trp, and the pyrrole moiety is still free to react [35].

A summary of the above observations, the predicted favorable initial reaction sites induced by h^+ and $^\bullet OH$ are different for some investigated cases. This may mean a mechanistic pathway difference for PC and PEC processes.

3.4. Photocatalytic and photoelectrocatalytic degradation products

The obtained FEDs calculation results suggested that PC and PEC may undergo different mechanistic pathways because of the different initial reaction site when a given amino acid is attacked by h^+ and $^\bullet OH$. If these FEDs predictions are true, then different intermediate products should be obtained from PC and PEC treated samples. Experiments were therefore carried out to determine the intermediate products of PC and PEC treated samples (see Figs. S4, S5, and 5). It should note that although the Waters 996 HPLC/MS was equipped with both PDA and ESI detectors, the attempt to directly identify the intermediates originated from the PC and PEC degradation of three model AAs based on ESI response was failed due to the high noisy to signal ratio. The same situation also occurred when the UPLC/MS/MS (Waters Xevo TQ, Micromass MS Technologies, UK) was used to identify their intermediates.

Fig. S4a shows the chromatograms of PC treated Phe solution. For samples without treatment, an absorption peak (Phe0) with a retention time (t_R) of 4.1 min was observed, signifying original Phe molecule. For 300 s PC treated sample, Phe1 (t_R = 3.5 min) was detected as earlier degradation intermediates. Phe1 was found to be more hydrophilic than that of Phe (Phe0). For 600 s PC treated sample, the Phe1 concentration in the reaction mixture was increased to approximately double of its concentration in 300 s PC treated sample mixture. When the treatment time was further increased, the Phe1 remains as an only dominant intermediate, and its concentration in the reaction mixture was increased gradually within 3000 s PC treatment. No new intermediate was detected within time interval investigated. The Phe1 which are more hydrophilic than Phe (Phe0) could be monohydroxylated or dihydroxylated or even trihydroxylated intermediate [38] as a result of $^\bullet OH$ attack on C^4 or C^7 (see $FED^2_{HOMO} + FED^2_{LUMO}$ value from Table 2). Fig. S4b shows the chromatograms of PEC treated Phe solution. An identical chromatogram was observed from the sample without treatment (Phe0). A more hydrophilic intermediate Phe2 (t_R = 3.4 min) than Phe1 was detected from PEC treated samples. It must mention that Phe2 is the only detected intermediate for PEC treatment. The intermediate Phe2 increased with the treatment time, reached its peak after 900 s of PEC treatment, and then its concentration in the reaction mixture was unchanged with further increase of the treatment time. It is also interesting to note that, according to the FEDs calculation results, although the reaction sites of Phe for electron extraction and radical attack are both located on the C^4 and C^7 (see Table 2), the intermediates of PC and PEC treatments are totally different. This could be one of the most important attributes that deviates the mechanistic pathways of PEC process from PC process.

Fig. S5 shows the chromatograms of PC and PEC treated Tyr samples. The original Tyr absorption peak (Tyr0) was observed at the retention time of 3.9 min. For PC treated samples (Fig. S5a), the concentration of Tyr decreased gradually with the increase of treatment time, and decreased to below the detection limit after 2400 s of PC treatment. At the same time, a dominant intermediate adsorption peak (Tyr1) with a retention time of 3.5 min was recorded. The intermediate Tyr1 was found to be more hydrophilic than Tyr and its concentration in the reaction mixture was increased as the treatment time increased. In addition, there were no other intermediates were observed. According to the reference [35], $^\bullet OH$ rapidly adds to the sites next to the original hydroxyl substituent at the side chain, followed by addition of an O_2 in the presence of oxygen. The subsequent elimination of peroxyl radical $HOO^\bullet$ leads to the final product, 3,4-dihydroxyphenylalanine. Multiple hydroxylations would generate trihydroxyphenylalanine. In the absence of oxygen, the primary product is still dihydroxyphenylalanine, but with a much low yield. Therefore, Tyr1 and Phe1, which have same retention time, are probable the same PC degraded intermediate, for instance, dihydroxyphenylalanine or trihydroxyphenylalanine. For PEC treated Tyr samples (Fig. S5b), Tyr1 is still a dominant intermediate with much higher concentration in comparison to the other new intermediates. In comparison to PC treated samples, Tyr1 produced only with PEC 150 s treatment, a new dominant intermediate of Tyr3 was detected with retention times of 3.3 min as PEC treatment time equal to or greater than 300 s, the concentration of Tyr3 in the reaction mixtures was rapidly increased when the treatment time was increased. This suggests that Tyr3

Table 2
Frontier electron densities (FEDs) on atoms of phenylalanine, tyrosine and tryptophan calculated by using Gaussian 03 Program.

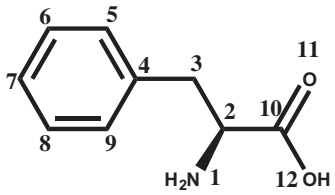

L-Phenylalanine

Atom	$2FED^2_{HOMO}$ h^+	$FED^2_{HOMO} + FED^2_{LUMO}$ $^{\bullet}OH$	Atom	$2FED^2_{HOMO}$ h^+	$FED^2_{HOMO} + FED^2_{LUMO}$ $^{\bullet}OH$
N^1	0.009	0.006	C^7	0.322	0.484
C^2	0.042	0.141	C^8	0.022	0.013
C^3	0.016	0.063	C^9	0.165	0.358
C^4	0.349	0.476	C^{10}	0.003	0.021
C^5	0.037	0.022	O^{11}	0.002	0.005
C^6	0.159	0.341	O^{12}	0.002	0.006

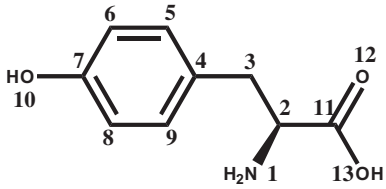

L-Tyrosine

Atom	$2FED^2_{HOMO}$ h^+	$FED^2_{HOMO} + FED^2_{LUMO}$ $^{\bullet}OH$	Atom	$2FED^2_{HOMO}$ h^+	$FED^2_{HOMO} + FED^2_{LUMO}$ $^{\bullet}OH$
N^1	0.008	0.015	C^8	0.106	0.325
C^2	0.047	0.065	C^9	0.089	0.413
C^3	0.013	0.042	O^{10}	0.223	0.112
C^4	0.359	0.184	C^{11}	0.002	0.009
C^5	0.040	0.291	O^{12}	0.001	0.002
C^6	0.173	0.422	O^{13}	0.001	0.002
C^7	0.230	0.119			

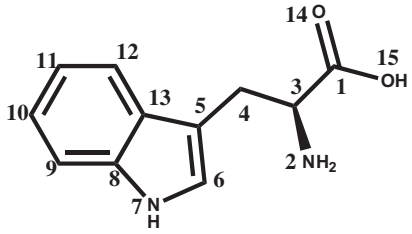

L-Tryptophan

Atom	$2FED^2_{HOMO}$ h^+	$FED^2_{HOMO} + FED^2_{LUMO}$ $^{\bullet}OH$	Atom	$2FED^2_{HOMO}$ h^+	$FED^2_{HOMO} + FED^2_{LUMO}$ $^{\bullet}OH$
C^1	0.002	0.007	C^9	0.140	0.350
N^2	0.011	0.008	C^{10}	0.164	0.269
C^3	0.046	0.030	C^{11}	0.010	0.031
C^4	0.007	0.006	C^{12}	0.181	0.383
C^5	0.292	0.210	C^{13}	0.038	0.120
C^6	0.227	0.334	O^{14}	0.001	0.001
N^7	0.168	0.122	O^{15}	0.002	0.002
C^8	0.046	0.028			

was produced from the further oxidation of intermediates. It is worth mentioning that Tyr3 is more hydrophilic than that of original Tyr molecule. In addition, two minor intermediates (Tyr2 and Tyr4) that are more hydrophobic than Tyr molecule were recorded at retention times of 7.5 min and 9.4 min, respectively. Tyr2 was found to be the minor intermediate for the sample subjected to 150 s PEC treatment and its concentration was rapidly deceased as the treatment time increased up to 300 s. It was also found that Tyr4 appeared when the treatment time was increased to 300 s, but rapidly decreased when the treatment time was further increased.

Fig. 5 shows the chromatograms of PC and PEC treated Trp samples. The absorption peak (Trp0) of original Trp molecule was observed at the retention time of 4.3 min. For PC treated samples (Fig. 5a), two major intermediates (Trp1 and Trp4) that are more hydrophilic than the original Trp molecule were detected with the retention times of 3.3 min and 3.6 min, respectively. Interestingly, no other detectable intermediates were recorded for PC treated samples. The intermediate Trp1 was observed from samples with treatment times of 600 and 1200 s by PC treatment. Its concentration was increased slightly as the treatment time increased and reduced to below the detection limit with the 1800 s of PC treatment. It should be noted that Trp (Trp0) concentration rapidly decreased as the formation of Trp1 occurred and reduced to below the detection limit when the reaction mixture was dominated

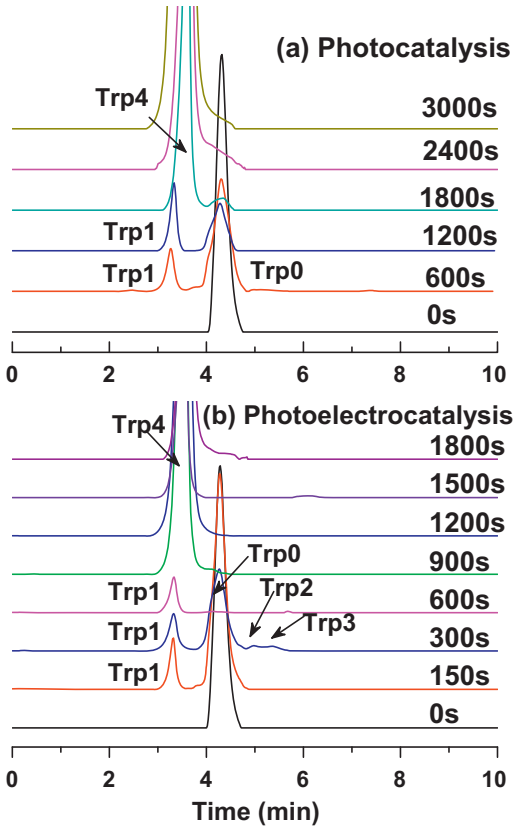

Fig. 5. The chromatograms obtained for PC (a) and PEC (b) treated tryptophan samples at different reaction intervals under 8.0 mW/cm^2 UV intensity. Initial concentration: 5.75 meq (N oxidized to NH_3); Applied potential bias for PEC: +0.30 V vs. Ag/AgCl; retention time: t_R(Trp0) = 4.3 min; t_R(Trp1) = 3.3 min; t_R(Trp2) = 5.0 min; t_R(Trp3) = 5.3 min; t_R(Trp4) = 3.6 min.

by the intermediate of Trp4 (2400 s PC treated sample). Other research [35] found that •OH is able to add to both benzene ring and pyrrole moiety. *N*-formylkynurenine and mono- and dihydroxytryptophan are the primary products of Trp. For PEC treated Trp samples (Fig. 5b), the original Trp molecule (Trp0) was completely consumed after 600 s PEC treatment. It was found that Trp1 (t_R = 3.3 min) became a minor intermediate with much lower concentration in comparison to PEC treated samples. Two intermediates (Trp2 and Trp3) that are more hydrophobic than the original Trp were recorded as minor intermediates. Both intermediates appeared only in 300 s PEC treated sample and rapidly decreased to below the detection level when the treatment time was greater than 600 s. Trp4 was recorded as the dominate intermediate for samples treated for 900 s or longer after intermediate Trp1 was disappeared. Its concentration in the reaction mixture was found to increase as the treatment time was increased even longer than 1800 s of PEC treatment. This suggests that Trp4 was the further oxidation product of reaction intermediates rather than the direct oxidation product of original Trp.

3.5. Mechanistic considerations

The experimental results showed above clearly demonstrated the oxidative degradation behavior (in teams of degradation efficiency and kinetics) differences among three AAs. These results of the oxidative degradation behavior differences between PC and PEC processes may be summarized as: For a given amino acid, the intermediates produced by PC and PEC treatments are different in terms of hydrophilicity; For a given treatment method (i.e., PC or PEC), the hydrophilicity characteristics of the intermediates produced are dependent on the type of AAs involved. Theoretically calculated $2FED^2_{HOMO}$ and $(FED^2_{HOMO} + FED^2_{LUMO})$ values (see Table 2) indicated that for a given amino acid, the initial reaction sites may be different for electron extraction (i.e., direct h^+ attack in PEC process) and radical attack (i.e., •OH in PC process). These predictions agreed well with the experimental results presented where for a given amino acid, PC and PEC differed remarkably from each other in terms of degradation efficiency (see Figs. 2–4) and degradation intermediates (see Figs. S4, S5 and 5). For a given treatment method (i.e., PC or PEC), the theoretically calculated $2FED^2_{HOMO}$ and $(FED^2_{HOMO} + FED^2_{LUMO})$ values of different AAs revealed that the initial reaction site are dependent on the type of AAs. For single-ringed amino acid such as Phe and Tyr, the initial reaction sites are likely to occur on the atoms within the 6-membered ring structure, regardless of the treatment process (e.g., via electron extraction in PEC process or radical attack in PC process). For double-ringed AAs such Trp, the initial reaction sites are likely to occur at 6-membered ring structure (PC process) or on 5-membered ring structure (PEC process).

The theoretical calculation and the experimental results obtained in this work suggested that the mechanistic pathway for PC and PEC processes might differ from each other. The differences degradation behaviors and products can be attributed to the different mechanistic pathways of PC and PEC processes. As aforementioned, according to reaction mechanisms reported to date, the photocatalytically produced intermediates should be exclusively more hydrophilic than its original amino acid molecules. This conclusion is agreed with our PC experimental data. However, production of intermediates more hydrophobic than their original AAs during PEC processes cannot be explained by any existing reaction mechanism. To date, no research has published to discuss PEC degradation mechanistic pathway of AAs. This means that the intermediates determined in this work need to be further examined and validated. In order to precisely determine PEC degradation reaction mechanism, the chemical structures of the produced intermediates must be precisely identified. A further systematic experimental work need carry out to achieve this. We are using preparative column to isolate sufficient qualities of intermediates for structural analyses by FT-IR, MS and NMR. The findings will be reported in near future.

4. Conclusion

In this work, the PC and PEC degradation of different AAs are systemically compared. A number of conclusions can be drawn based on the obtained experimental results: For a given amino acid, PEC method possesses higher degradation efficiency than that of PC method. The superiority of PEC over PC method becomes more obvious at higher concentrations. For a given amino acid, the hydrophilicity characteristics of PC produced intermediates are differed slightly from those of PEC produced intermediates except Phe. For a given method, similar hydrophilicity characteristics were obtained from all AAs investigated except Phe. For a given amino acid, the theoretically calculated $2FED^2_{HOMO}$ and $(FED^2_{HOMO} + FED^2_{LUMO})$ values suggest that the initial reaction sites are different for PC and PEC processes, which agreed well with the experimental results. For a given method, the theoretically calculated $2FED^2_{HOMO}$ and $(FED^2_{HOMO} + FED^2_{LUMO})$ values of different AAs suggest that the initial reaction sites for all single-ringed AAs are likely to occur on the atoms within 6-membered ring structure, while for double-ringed amino acid, the initial reaction sites are likely to occur at 6-membered ring structure (PC process) or on 5-membered ring structure (PEC process). Both theoretical calculation and experimental results suggest that the mechanistic pathway of PEC process differs from that of PC process. Further

experimental work will be completed to identify the precise chemical structures of the produced intermediates, allowing a precise description of reaction mechanism.

Acknowledgments

This is contribution No. IS–1902 from GIGCAS. This work was supported by Australian Research Council and NSFC (no. 21077104), Knowledge Innovation Program of Guangzhou Institute of Geochemistry, CAS (GIGCX-10-01).

Appendix A. Supplementary data

Supplementary data associated with this article can be found, in the online version, at http://dx.doi.org/10.1016/j.cattod.2014.05.040.

References

[1] M. Matsushita, T.H. Tran, A.Y. Nosaka, Y. Nosaka, Catal. Today 120 (2007) 240–244.
[2] Y. Chen, G.P. Yang, G.W. Wu, X.C. Gao, Q.Y. Xia, Cont. Shelf Res. 52 (2013) 97–107.
[3] A. Dotson, P. Westerhoff, J. Am, Water Works Assoc. 101 (2009) 101–115.
[4] E.M. Casbeer, V.K. Sharma, Z. Zajickova, D.D. Dionysiou, Environ. Sci. Technol. (2013), http://dx.doi.org/10.1021/es305283k
[5] A.Y. Nosaka, G. Tanaka, Y. Nosaka, J. Phys. Chem. B 116 (2012) 11098–11102.
[6] J. Méndez-Hurtado, R. López, D. Suárez, M.I. Menéndez, Chem. Eur. J. 18 (2012) 8437–8447.
[7] M. Malis, Y. Loquais, E. Gloaguen, H.S. Biswal, F. Piuzzi, B. Tardivel, V. Brenner, M. Broquier, C. Jouvet, M. Mons, N. Doslic, I. Ljubic, J. Am. Chem. Soc. 134 (2012) 20340–20351.
[8] E. Szabo-Bardos, K. Somogyi, N. Toro, G. Kiss, A. Horvath, Appl. Catal. B: Environ. 101 (2011) 471–478.
[9] L. Elsellami, F. Vocanson, F. Dappozze, E. Puzenat, O. Paisse, A. Houas, C. Guillard, Appl. Catal. A: Gen. 380 (2010) 142–148.
[10] X. Yao, G.W. Zhu, L.L. Cai, M.Y. Zhu, L.L. Zhao, G. Gao, B.Q. Qin, Aquat. Geochem. 18 (2012) 263–280.
[11] P. Menzel, B. Gaye, M.G. Wiesner, S. Prasad, M. Stebich, B.K. Das, A. Anoop, N. Riedel, N. Basavaiah, Limnol. Oceanogr. 58 (2013) 1061–1074.
[12] N. Kawasaki, K. Komatsu, A. Kohzu, N. Tomioka, R. Shinohara, T. Satou, F.N. Watanabe, Y. Tada, K. Hamasaki, M.R.M. Kushairi, A. Imai, Appl. Environ. Microbiol. (2013), http://dx.doi.org/10.1128/AEM.01504-01513
[13] C. Na, T.M. Olson, Environ. Sci. Technol. 41 (2007) 3220–3225.
[14] M. Deborde, U. von Gunten, Water Res. 42 (2008) 13–51.
[15] A.D. Shah, W.A. Mitch, Environ. Sci. Technol. 46 (2012) 119–131.
[16] E.C. Wert, F.L. Rosario-Ortiz, Environ. Sci. Technol. 47 (2013) 6332–6340.
[17] X. Yang, C.H. Fan, C.I. Shang, Q. Zhao, Water Res. 44 (2010) 2691–2702.
[18] M.R. Hoffmann, S.T. Martin, W.Y. Choi, D.W. Bahnemann, Chem. Rev. 95 (1995) 69–96.
[19] S. Malato, P. Fernandez-Ibanez, M.I. Maldonado, J. Blanco, W. Gernjak, Catal. Today 147 (2009) 1–59.
[20] J.L. Wang, L.J. Xu, Crit. Rev. Environ. Sci. Technol. 42 (2012) 251–325.
[21] T.H. Tran, A.Y. Nosaka, Y. Nosaka, J. Phys. Chem. B 110 (2006) 25525–25531.
[22] M.R.V. Sahyun, N. Serpone, J. Photochem. Photobiol. A 115 (1998) 231–238.
[23] S. Horikoshi, N. Serpone, J.C. Zhao, H. Hidaka, J. Photochem. Photobiol. A 118 (1998) 123–129.
[24] H. Hidaka, E. Garcia-Lopez, L. Palmisano, N. Serpone, Appl. Catal. B: Environ. 78 (2008) 139–150.
[25] S. Horikoshi, H. Hidaka, J. Photochem. Photobiol. A 141 (2001) 201–207.
[26] H. Hidaka, S. Horikoshi, K. Ajisaka, J. Zhao, N. Serpone, J. Photochem. Photobiol. A 108 (1997) 197–205.
[27] M.A. Fox, M.J. Chen, J. Am. Chem. Soc. 105 (1983) 4497–4499.
[28] J. Monig, R. Chapman, K.D. Asmus, J. Phys. Chem. 89 (1985) 3139–3144.
[29] S.Q. Zhang, D.L. Jiang, H.J. Zhao, Environ. Sci. Technol. 40 (2006) 2363–2368.
[30] H.J. Zhao, D.L. Jiang, S.Q. Zhang, W. Wen, J. Catal. 250 (2007) 102–109.
[31] H.J. Zhao, D.L. Jiang, S.Q. Zhang, K. Catterall, R. John, Anal. Chem. 76 (2004) 155–160.
[32] G.Y. Li, Y.L. Zhang, H.W. Sun, J.B. An, X. Nie, H.J. Zhao, P.K. Wong, T.C. An, Catal. Today 201 (2013) 167–174.
[33] Y. Ohko, K.I. Iuchi, C. Niwa, T. Tatsuma, T. Nakashima, T. Iguchi, Y. Kubota, A. Fujishima, Environ. Sci. Technol. 36 (2002) 4175–4181.
[34] X. Zhang, F. Wu, X.W. Wu, P.Y. Chen, N.S. Deng, J. Hazard. Mater. 157 (2008) 300–307.
[35] G.H. Xu, M.R. Chance, Chem. Rev. 107 (2007) 3514–3543.
[36] K. Nohara, H. Hidaka, E. Pelizzetti, N. Serpone, J. Photochem. Photobiol. A 102 (1997) 265–272.
[37] X.L. Zhu, C.W. Yuan, Y.C. Bao, J.H. Yang, Y.Z. Wu, J. Mol. Catal. A: Chem. 229 (2005) 95–105.
[38] G.Z. Xu, M.R. Chance, Anal. Chem. 77 (2005) 4549–4555.